

# OVERCOMING HYDROPHONE POSITION INACCURACY IN CONVENTIONAL BEAMFORMING

Dr G.D.Quartly (1) & Dr N. G. Pace (2)

(1) RSADU, James Rennell Centre for Ocean Circulation, Chilworth Research Park,

(2) School of Physics, University of Bath, Bath, Avon [ Southampton

## 1. INTRODUCTION

Passive sensing using a towed array of hydrophones has long been an important tool in the detection of submarines. The signals received by the hydrophones are delayed relative to one another due to the different transmission times from source to receivers. All methods of detecting and locating sources from these signal records rely on appropriate delays being applied to these simultaneous records to compensate for those due to the expected bearing of the source. The simplest of these, Conventional Beamforming (CBF), just adds these suitably delayed signals together and squares the result to give a positive value corresponding to the power perceived from a direction. More complicated non-linear methods exist which examine the structure of the cross-correlation matrix; these are not dealt with here.

All methods are sensitive to noise in the data or errors in the model assumed. Additive noise can be due to other submarines or ships (including that towing the array), sea creatures, wind, wave-breaking and all forms of precipitation, as well as noise generated by dragging the array through the water. Model errors may be failure to allow for correlated sources, near-field sources, fluctuations in the transmission medium, multipath propagation and poorly determined sensor locations. This work concentrates on the effect of the last of these on Conventional Beamforming, although some account is taken of the other sources of error.

## 2. DEGRADATION OF ARRAY PERFORMANCE

Typical output of a simulation of CBF processing is shown in Fig 1a, where a single source at broadside was considered and no noise effects were present. The beam pattern displayed, with the ordinate scaled in decibels, has a multi-lobed structure with the main peak corresponding to the bearing of the source, but other (lower) peaks being an artefact of the process rather than indicating extra sources. [ If there had been ambient noise in the simulation, it would have added a continuum to the beam pattern obliterating any information on lobes weaker than its level. ]

If the array had a slight bow in its shape of amplitude  $0.3\lambda$  (where  $\lambda$  is the wavelength of the sound waves processed), but processing was done for a straight array then the beam pattern would be degraded as in Fig 1b. [ The 'bow' used here is half a sinusoidal wave; Hodgkiss<sup>1</sup> obtained similar results using a circular arc. ] A much more severe deformation of amplitude  $\lambda$  results in the beam pattern shown in Fig 1c, where the mainlobe (that in the direction of the source) has diminished to a level below that of the subsidiary sidelobes. If significant noise was also present, only the top 2 peaks might be discernible so that two sources would be perceived to exist at  $\sim 15^\circ$  to broadside rather than the solitary one at  $0^\circ$  which is correct. If the beamforming operation is performed using the true sensor locations i.e. same as in the simulations, then a pattern similar to Fig 1a would be achieved. Thus it can be seen to be very important to determine the appropriate sensor positions to be used.

## OVERCOMING HYDROPHONE POSITION UNCERTAINTY

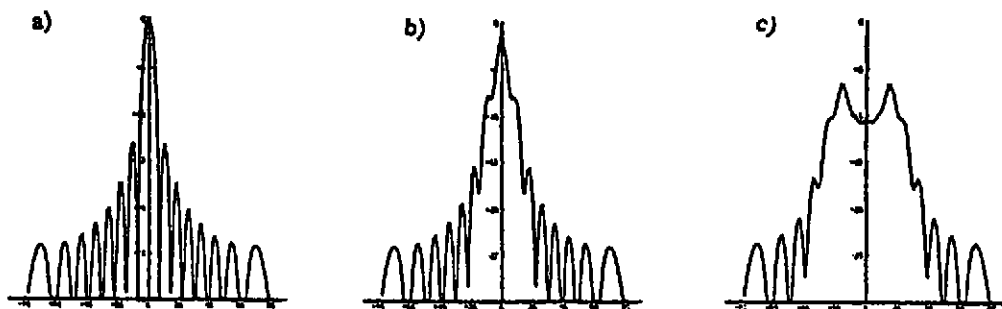


Fig 1 : a) Typical output of CBF processing using an array of 16 elements at  $\lambda/2$  separation and a source at  $0^\circ$ . [ Angular span is  $-90^\circ$  to  $90^\circ$ ; y-axis has a range of 30dB. ] b) Beam pattern produced when array has a bow in it of amplitude  $0.3\lambda$ , but is processed as though straight. c) Same as for b) but with bow of size  $\lambda$ .

### 3. USE OF POWER FUNCTIONS TO MONITOR FOCUSING OF ARRAY

#### 3.1 Definition of Power Function, $\Phi$

Following the work of Muller & Buffington<sup>2</sup> and Bucker<sup>3</sup>, it was decided to pursue an approach based on evaluating some measure of the 'sharpness' or focusing achieved by the processing. A suitable function, here denoted by  $\Phi$ , is the square of the power perceived from an angle, weighted by a  $\cos\theta$  term and integrated (usually  $-90^\circ$  to  $90^\circ$  relative to broadside, but it can be for a full  $360^\circ$ ) viz:-

$$\Phi = \int p^2(\theta) \cos\theta \, d\theta \approx \sum_i^N p_i^2 \cos\theta_i \quad (1)$$

where  $p_i = p(\theta_i)$ . Other power functions, involving terms such as  $p_i^3$  have been tested<sup>4</sup>, but this is the simplest and is found to perform well. It can be related to the variation of power levels in the beam pattern about a mean uninformative level:-

$$\Phi = \sum [ p_i - P ]^2 \cos\theta_i + \sum P^2 \cos\theta_i \quad (2)$$

where  $P = \{ \sum p_i \cos\theta_i \} / \{ \sum \cos\theta_i \}$  is the (weighted) mean of  $p_i$ . [ Value  $P$  is related to the total power in the pattern and is approximately independent of the processing shape used. ]

If a signal record is simulated for a bow of a certain amplitude and CBF applied to different estimates of the sensor positions corresponding to different amplitude deformations of the array, then the beam pattern will evolve through the patterns shown in Figs 1c,1b,1a and back through Figs 1b,1c again; the power function,  $\Phi$ , will change smoothly, showing a maximum for zero error in the sensor positions [Fig 2a]. Thus for small errors in the size of the bow, an examination of the local gradient of  $\Phi$  with respect to bow size will infer the necessary direction

## OVERCOMING HYDROPHONE POSITION UNCERTAINTY

of change of the size. If large errors in this size are considered, the variation of  $\Phi$  is as in Fig 2b. This shows that the variation does not have a single peak; thus convergence to true via a gradient routine can only be assured for an error,  $\Delta a_1$ , in the range  $-3\lambda < \Delta a_1 < 3\lambda$ .

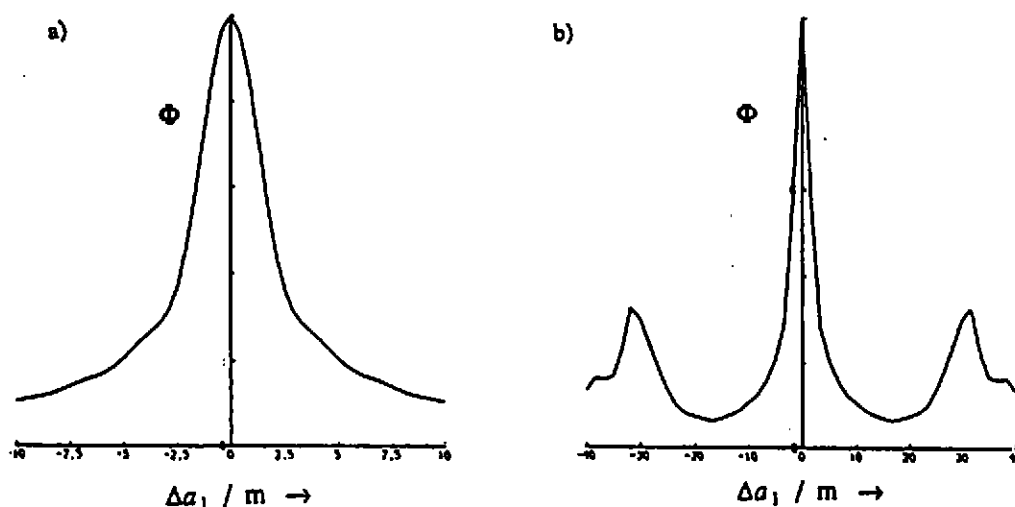


Fig 2 : a) Variation of power function,  $\Phi$  with error in estimate of  $a_1$ . [ Example is for  $\lambda=6m$  and a 16 element array of length 45m. ] b) Same as for a) but on a larger scale to illustrate minima and secondary maxima.

### 3.2 Generalized Deformation of Array Shape

A bow-like deformation of the array may be the most likely intuitively — either due to towing ship undergoing cornering manoeuvre or presence of a strong current across the array — but array shapes of a different nature may also be envisaged e.g. due to transverse waves propagating along the array. As an example of such snaking of the array, the array shape was also modeled as a full sinusoidal wave [Fig 3a]. The degradation of the beam pattern resulting from errors of this nature of amplitude  $0.2\lambda$  and  $0.5\lambda$  are shown in Figs 3b,c respectively. It is found that  $\Phi$  as defined previously, still shows a smooth variation with a maximum for zero error. In this case, the minima in the power function plot are nearer, so that convergence via a slope following approach is only guaranteed if the error in this second term,  $\Delta a_2$  is in the range  $-\lambda < \Delta a_2 < \lambda$ . Further work has shown that use of higher order sinusoids still causes the power function to vary in a smooth manner with a maximum for zero error.

## OVERCOMING HYDROPHONE POSITION UNCERTAINTY

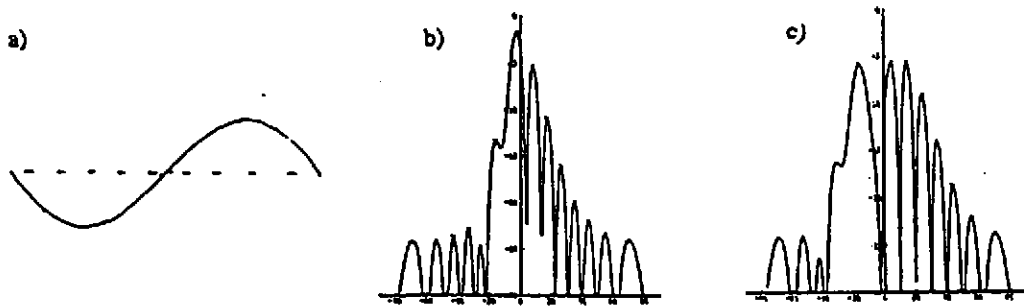


Fig 3 : a) Full sinusoidal deformation of array. b) Beam pattern for errors in array shape as in a) of amplitude  $0.2\lambda$ . c) Same as b) but for  $0.5\lambda$ .

### 3.3 Effect of Noise on the Performance of $\Phi$

Random additive noise affects this simplistic idea of a well defined maximum of  $\Phi$  lying at the location corresponding to zero location error. Moderate levels of noise are found to cause significant secondary maxima in  $\Phi$  to occur and also to shift the position of the main peak. Fig 4 shows a few simulations with an input noise level of equal strength to the source. Now use of a routine to locate the value with maximum  $\Phi$  will converge to one of those peaks leading to an error in the estimation of  $a_1$ . The beam pattern formed using such a selected array shape will no longer show a mainlobe exactly in the direction of the source, although at this level the error is mainly due to the presence of the noise itself rather than the indeterminacy in the array sensor locations.

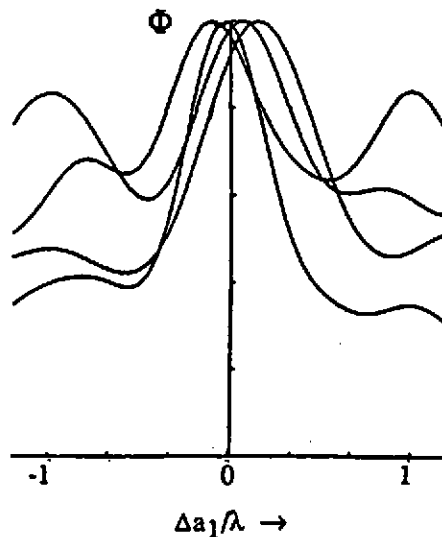


Fig 4 : Four plots of variation of  $\Phi$  with  $a_1$  for a 16 element array with an input SNR of 0dB showing the displacement of the peak and the greater proximity of secondary maxima.

## OVERCOMING HYDROPHONE POSITION UNCERTAINTY

It is instructive to examine the error in the estimate of  $a_1$  due to the noise i.e. the typical displacement of the peak of  $\Phi$ . Many repeated simulations with noise uncorrelated between sensors shows the displacements of the maximum of  $\Phi$  to possess a normal distribution about zero error. Representing the error in estimating the coefficient of  $a_1$  by  $\sigma(a_1)$  (the standard deviation of the spread of estimates), simulations show that:-

$$\sigma(a_1)/\lambda \approx \frac{0.37 \sec\theta}{\sqrt{n \cdot p_s/p_n}} \quad (3)$$

where  $\theta$  is the bearing of the source,  $n$  is the no. of elements and  $p_s/p_n$  is the signal to noise ratio on input. A similar expression holds for errors in estimation of  $a_2$ , but with the coefficient changed to 0.25 due to the different shape of the deformation. A theoretical justification of this relationship is given in reference 4.

Good agreement was found between equation 3 and simulation work for a wide range of conditions — input SNR from 45dB to 0dB, no. of elements in the range 8 to 32 and source bearings from  $0^\circ$  to  $50^\circ$ . The shape estimator was found to perform poorer than expected for very low and very high noise levels [see Fig 5]; under the former regime errors were larger due to numerical problems associated with beamforming at discrete angles and the limited holding accuracy of the computer, whilst under the latter the signal was too weak for the algorithm to cope. Further difficulties were encountered when the source bearing was more than  $60^\circ$  from broadside. Most of the work was done using an array with elements at  $\lambda/2$  spacing, but equation 3 holds true for a range of element separations, although if separation is too large effects due to aliasing can cause problems. Only a little work was done for arrays of more than 32 elements; indications are that performance continues as predicted.

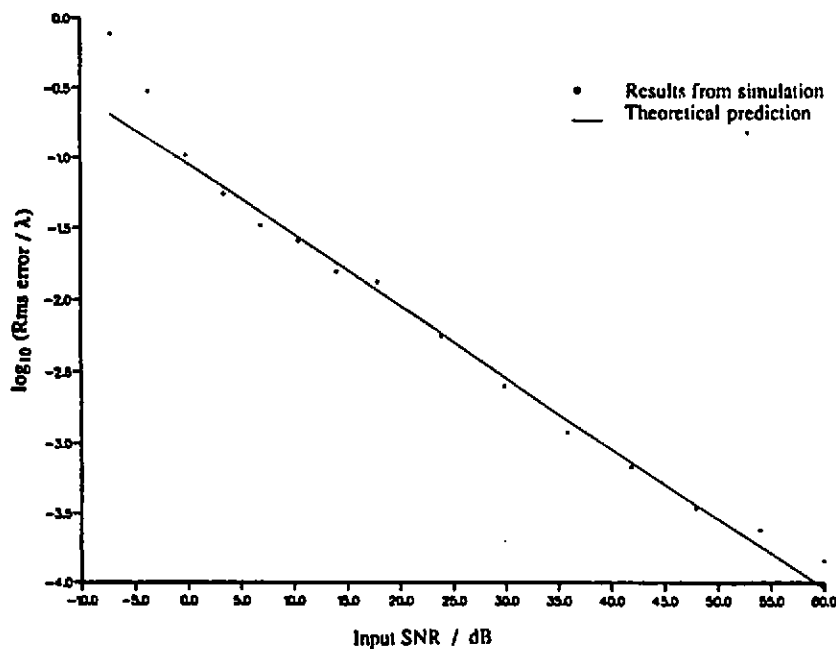


Fig 5 : Plot of estimation accuracy of  $a_1$  against input Signal to Noise Ratio.

# OVERCOMING HYDROPHONE POSITION UNCERTAINTY

## 4. CONVERGENCE PROPERTIES OF SHAPE ESTIMATOR

### 4.1 Ideal Conditions

The shape of the array under realistic conditions may be expressed as the sum of such sinusoidal components. In general  $n$  components would be required for an array of  $n$  elements, but the physical constraints of a towed array under tension imply that the coefficients for the higher order values may be set to zero without appreciable loss in performance. Expansion of the shape as a Fourier Series thus reduces the number of parameters to be estimated from  $n$  to  $k$  (the no. of Fourier terms required). The value of  $k$  will depend upon the array length expressed in  $\lambda$  and the towing conditions, but it is probably of the order of 4 to 8 for most purposes; the paragraphs below use a value of 2 as this is easiest for visualization purposes.

Even with only 4 parameters, a grid type search over all unknowns at high resolution would be computationally very intensive. However, the smooth nature of the  $\Phi$ -surface as portrayed in Figs 2a,6a lends itself to utilization of a simple gradient climbing routine. In the case illustrated in Fig 6a, convergence can be seen to be straight forward for any starting estimate for which  $a_1$  and  $a_2$  are within  $\lambda$  of true.

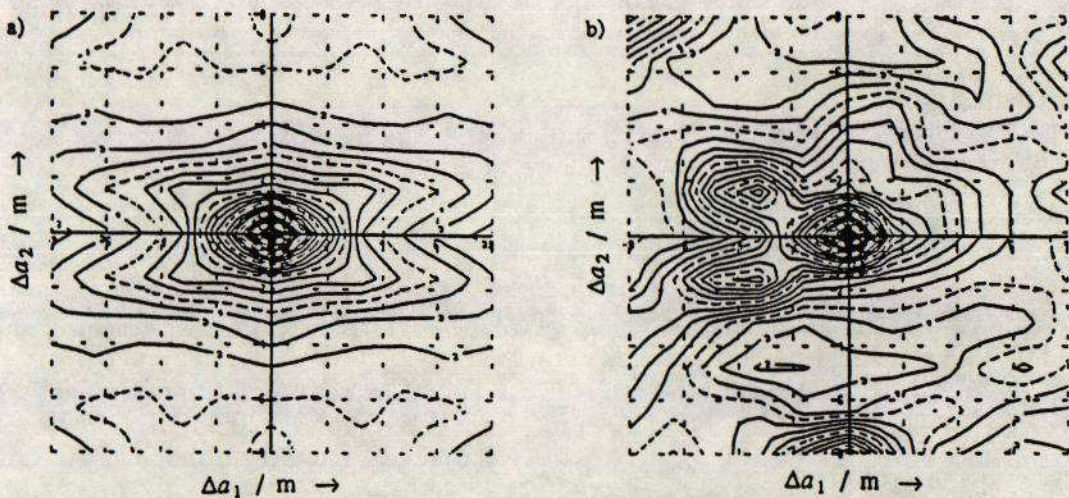


Fig 6 : a) Variation of  $\Phi$  with  $a_1$  and  $a_2$  with no noise present. [ Example is for  $a_1, a_2$  in the range  $-8m$  to  $8m$  with  $\lambda=6m$ . ] b) Same for a particular realization with significant noise (3dB less than signal strength)

### 4.2 Convergence in the Presence of Noise

Addition of significant noise into the simulation not only affects the location of the peak point (corresponding to a shape error when the image is 'sharpest') but also causes the formation of subsidiary maxima much nearer than in the no noise case [cf Figs 2a, 4]. An example is shown in Fig 6b; gradient climbing routines may easily converge to such subsidiaries resulting in a poorly focused image being selected. As this is merely a product of processing random noise on top of a signal, these extra points are not constant in location, but may occur anywhere on the lower contours of the main peak. The higher the noise level, the nearer these spurious peaks may occur

## OVERCOMING HYDROPHONE POSITION UNCERTAINTY

to true and thus the smaller the convergence region. Application of Hamming weights at the beamforming stage proves beneficial as it reduces the prominence of spurious peaks in the  $a_1$ - $a_2$  plane; however use of such shading does also increase the error in the location of the main peak.

### 5. SUMMARY

This paper has examined the problems endemic in sonar processing due to uncertainties in sensor positions. The resultant degradation to output of Conventional Beamforming has been illustrated and a tool introduced which helps deduce sensor positions (and thus source bearings) in a computationally simple manner. This work expands on that of others<sup>2,3</sup> in that it derives the limits on such a task, showing how they depend on the signal record (strength of signal relative to background noise and source bearing) and on array characteristics (no. of elements, their separation and the wavelength of sound processed).

Another facet of the shape determining problem was also explored, that of the region in parameter space for which convergence to true is fairly straightforward. The false 'focusing points' introduced by noise were demonstrated, although it was emphasised that none of these are constant in location, merely being an artefact of processing a particular realization of the noise field. The effect of applying weights to the elements at the beamforming stage was also discussed.

### Acknowledgements

The authors are grateful for the financial support given by BAe SEMA (formerly CAP Scientific) for the research studentship under which the work originated.

### 6. REFERENCES

- [1] W.S.HODGKISS 'The Effects of Array Shape Perturbation on Beamforming and Passive Ranging' *J Ocean Eng* 8, 120-130 (1983)
- [2] R.A. MULLER & A. BUFFINGTON 'Real-Time Correction of Atmospherically Degraded Telescope Images through Image Sharpening', *J Opt Soc Am* 64, 1200-1210 (1974)
- [3] H.P.BUCKER 'Beamforming a Towed Line Array of Unknown Shape', *J Acoust Soc Am* 63, 1451-1454 (1978)
- [4] G.D.QUARTLY 'An Investigation into the Deterioration of Source Detection due to Positional Uncertainty, and of How it Might be Remedied' PhD thesis, School of Physics, University of Bath (1989)